sustainability

MDPI

Article

Adsorption/Desorption Capability of Potassium-Type Zeolite Prepared from Coal Fly Ash for Removing of Hg^{2+}

Yuhei Kobayashi [1], Fumihiko Ogata [1], Chalermpong Saenjum [2,3], Takehiro Nakamura [1] and Naohito Kawasaki [1,4,*]

[1] Faculty of Pharmacy, Kindai University, 3-4-1 Kowakae, Higashi-Osaka, Osaka 577-8502, Japan; 1944420001t@kindai.ac.jp (Y.K.); ogata@phar.kindai.ac.jp (F.O.); nakamura@phar.kindai.ac.jp (T.N.)
[2] Faculty of Pharmacy, Chiang Mai University, Suthep Road, Muang District, Chiang Mai 50200, Thailand; chalermpong.saenjum@gmail.com
[3] Cluster of Excellence on Biodiversity-based Economics and Society (B.BES-CMU), Chiang Mai University, Suthep Road, Muang District, Chiang Mai 50200, Thailand
[4] Antiaging Center, Kindai University, 3-4-1 Kowakae, Higashi-Osaka, Osaka 577-8502, Japan
* Correspondence: kawasaki@phar.kindai.ac.jp; Tel.: +81-6-4307-4012

Abstract: The feasibility of using potassium-type zeolite (K-type zeolite) prepared from coal fly ash (CFA) for the removal of Hg^{2+} from aqueous media and the adsorption/desorption capabilities of various potassium-type zeolites were assessed in this study. Potassium-type zeolite samples were synthesized by hydrothermal treatment of CFA at different intervals (designated CFA, FA1, FA3, FA6, FA12, FA24, and FA48, based on the hours of treatment) using potassium hydroxide solution, and their physicochemical characteristics were evaluated. Additionally, the quantity of Hg^{2+} adsorbed was in the order CFA, FA1 < FA3 < FA6 < FA12 < FA24 < FA48, in the current experimental design. Therefore, the hydrothermal treatment time is important to enhance the adsorption capability of K-type zeolite. Moreover, the effects of pH, temperature, contact time, and coexistence on the adsorption of Hg^{2+} were elucidated. In addition, Hg^{2+} adsorption mechanism using FA48 was demonstrated. Our results indicated that Hg^{2+} was exchanged with K^{+} in the interlayer of FA48 (correlation coefficient = 0.946). Finally, adsorbed Hg^{2+} onto FA48 could be desorbed using a sodium hydroxide solution (desorption percentage was approximately 70%). Our results revealed that FA48 could be a potential adsorbent for the removal of Hg^{2+} from aqueous media.

Keywords: hydrothermal activation treatment; recycling technology; heavy metal; ion exchange

Citation: Kobayashi, Y.; Ogata, F.; Saenjum, C.; Nakamura, T.; Kawasaki, N. Adsorption/Desorption Capability of Potassium-Type Zeolite Prepared from Coal Fly Ash for Removing of Hg^{2+}. *Sustainability* **2021**, *13*, 4269. https://doi.org/10.3390/su13084269

Academic Editors: Mohd Rafatullah and Masoom Raza Siddiqui

Received: 10 March 2021
Accepted: 9 April 2021
Published: 12 April 2021

1. Introduction

The 2030 agenda for sustainable development, such as clean water and sanitation (Goal 6) and life below water (Goal 14), were adopted by all member states of the United Nations in 2015 [1], to establish a sustainable society, which is a matter of global concern. In particular, heavy metal pollution has become a severe global environmental issue, including in the developing countries. Among them, mercury (Hg^{2+}), lead (Pb^{2+}), and cadmium (Cd^{2+}) are referred to as the "big three" heavy metals with the greatest potential risk to human health and water environment [2–4]. They are highly toxic to organisms [5]. Mercury (Hg) and its compounds can cause serious threats to organisms, including humans, because of their bioaccumulative properties, damaging the bones, liver, kidney, and nervous system [6–8]. The Minamata Convention on Mercury was adopted by the Intergovernmental Negotiating Committee in 2017. The International Agency for Research on Cancer categorizes methylmercury compounds as group 2B (possibly carcinogenic to humans), and metallic Hg and inorganic Hg compounds as group 3 (unclassifiable as to carcinogenicity in humans) [9]. In addition, the maximum permissible limit of Hg in drinking water as recommended by the U.S. Environmental Protection Agency and many

countries are 2 μg/L and 1 μg/L, respectively [7,10,11]. Therefore, removal of Hg^{2+} from aqueous media is crucial for human health and conservation of the water environment.

Coal is one of the most abundant energy sources worldwide [12]. A previous study reported that the global trend of increasing energy production continued in 2018 [13]. In addition, it is desirable to increase coal-fired power generation by up to 46% of the total electricity production by 2030 [14]. Additionally, the demand for coal-fired power plants has increased after the Fukushima Daiichi Nuclear Power Station disaster (2017) in Japan. Accordingly, approximately 800–900 million ton per year of coal fly ash (CFA), a by-product from the combustion of coal, is generated worldwide. Although the CFA has been recycled as supplements for cement, concrete, soil conditioners, and fertilizer materials [15–17], a major portion has been disposed of in landfills. Thus, from the perspective of a sustainable society, it is necessary to develop a recycling technology for CFA.

In this study, we focused on the preparation and production of zeolites from CFA. The CFA, characterized by aluminosilicate and silicon phases, is a superior material for zeolite synthesis [18]. Zeolite is a microporous crystalline hydrated aluminosilicate characterized by a three-dimensional network of tetrahedral (aluminum and silicon) O4 units that form a system of interconnected pores [18]. The applications of CFA derived zeolite are well-known. They have been used for heavy metal removal from aqueous media [19,20], as well as for the remediation of acid mine drainage [21,22]. Thus, this conversion of CFA to zeolite is useful for the development of a sustainable society as it decreases the waste generated from coal-fired power plants. Many conversion technologies, namely fusion-assisted hydrothermal treatment [14], multi-step treatment [14], sonication [14], conventional hydrothermal treatment [23,24], and microwave irritation [25,26] have been reported in previous studies. Zeolite synthesis involves three steps: dissolution, condensation, crystallization [27]. Among the technologies, conventional hydrothermal treatment is comparatively simple and inexpensive [23].

Previously, we reported that potassium-type zeolite (K-type zeolite) prepared from CFA had characteristic physicochemical properties and showed potential in heavy metal adsorption from aqueous media [28]. In addition, previous studies have assessed the adsorption capacity and mechanism of Hg^{2+} removal using CFA [29]. However, there are no reports on the adsorption of Hg^{2+} using potassium-type zeolites prepared from CFA using conventional hydrothermal treatment. Thus, if potassium-type zeolite could be explored for the removal of Hg^{2+} from aqueous media, this alternative would contribute considerably to the waste reduction from coal-fired power plants or water conservation.

This study aimed to investigate the possibility of Hg^{2+} removal from aqueous media using K-type zeolite prepared from CFA. The effects of pH, temperature, contact time, coexistence, and selectivity on the adsorption of Hg^{2+} were assessed.

2. Materials and Methods

2.1. Materials

The standard solution of Hg^{2+} ($HgCl_2$ in 0.1 mol/L HNO_3) was purchased from FUJIFILM Wako Pure Chemical Co., Osaka, Japan. Coal fly ash (CFA) was obtained from the Tachibana-wan Power Station (Shikoku Electric Power, Inc., Tokushima, Japan). Additionally, the standard solutions of Na^+ (NaCl in water), Mg^{2+} ($Mg(NO_3)_2$ in 0.1 mol/L HNO_3), K^+ (KCl in water), Ca^{2+} ($CaCO_3$ in 0.1 mol/L HNO_3), Ni^{2+} ($Ni(NO_3)_2$ in 0.1 mol/L HNO_3), Cu^{2+} ($Cu(NO_3)_2$ in 0.1 mol/L HNO_3), Zn^{2+} ($Zn(NO_3)_2$ in 0.1 mol/L HNO_3), Sr^{2+} ($SrCO_3$ in 0.1 mol/L HNO_3), and Cd^{2+} ($Cd(NO_3)_2$ in 0.1 mol/L HNO_3) were also obtained from FUJIFILM Wako Pure Chemical Co., Osaka, Japan. Potassium-type zeolite (K-type zeolite) was prepared by hydrothermal activation treatment using CFA in potassium hydroxide solution [28]. Three grams of CFA was mixed with 3 mol/L potassium hydroxide solution (240 mL). The mixture solution was heated at 93 °C for 1(FA1), 3(FA3), 6(FA6), 12(FA12), 24(FA24), and 48(FA48) h, followed by filtering through a 0.45 μm membrane filter (Advantec MFS, Inc., Tokyo, Japan) [30]. The residue was washed with distilled water and dried at 50 °C for 24 h. Potassium hydroxide, nitric acid, and sodium hydroxide were

purchased from FUJIFILM Wako Pure Chemical Co. (Osaka, Japan). All reagents were of special grade.

We had previously reported the physicochemical characteristics of K-type zeolites [28]. X-ray diffraction (XRD) and morphology analyses were performed using MiniFlex II (Rigaku, Osaka, Japan) and SU1510 (Hitachi High-Technologies Co., Tokyo, Japan), respectively. The cation exchange capacity (CEC) and pH_{pzc} were measured using the Japanese Industrial Standard Method (JIS K 1478) and the method previously reported by Faria et al. [31]. Additionally, the specific surface area and pore volume were measured using NOVA4200*e* (Quantachrome Instruments Japan G.K., Tokyo, Japan). The binding energy was measured using a JXA-8530F (JEOL Ltd., Tokyo, Japan). Finally, the solution pH was measured using an F-73S digital pH meter (HORIBA, Ltd., Kyoto, Japan).

2.2. Amount of Hg^{2+} Adsorbed Using FA Series

Approximately 0.01 g of each pretreated adsorbent, namely CFA, FA1, FA3, FA6, FA12, FA24, and FA48, was mixed with 50 mL of 50 mg/L Hg^{2+} solution. Subsequently, the reaction mixture was shaken at 100 rpm and 25 °C for 24 h. The resulting sample was filtered through a 0.45 μm membrane filter. The concentration of Hg^{2+} was measured using an inductively coupled plasma optical emission spectrometer (iCAP-7600 Duo, Thermo Fisher Scientific Inc., Osaka, Japan). The quantity of Hg^{2+} adsorbed was calculated using the levels before and after adsorption in Equation (1).

$$q = \frac{(C_0 - C_e)V}{W} \quad (1)$$

where q is the quantity adsorbed (mg/g); C_0 is the initial concentration (mg/L); C_e is the equilibrium concentration (mg/L); V is the solvent volume (L); and W is the weight of the adsorbent (g).

2.3. Effect of pH, Temperature, and Contact Time on the Adsorption of Hg^{2+}

First, in order to evaluate the effect of pH, FA48 (0.01 g) was added to 50 mL of the Hg^{2+} solution at 10, 30, 50 mg/L. The pH of the solution was adjusted to 2, 5, 7, 9, 11 using either nitric acid or sodium hydroxide solutions. The suspension was shaken at 100 rpm at 25 °C for 24 h, and filtered using a 0.45 μm membrane filter. Second, in order to evaluate the temperature effect, FA48 (0.01 g) was added to a 50 mL Hg^{2+} solution at 10, 20, 30, 40, 50 mg/L, and the suspension was shaken at 100 rpm at 7, 25, 45 °C for 24 h. The 7 °C of solution was prepared as follows. The sample solution was set at 5 °C in a water bath shaker personal-11 (TAITEC Co., Nagoya, Japan) in the low-temperature room at 6 °C. Finally, to evaluate the effect of contact time, FA48 (0.01 g) was added to 50 mg/L Hg^{2+} solution (50 mL). The suspension was shaken at 100 rpm and 25 °C for 0.5, 1, 3, 6, 12, 18, 21, 24, 30, 42, 48 h. The amount of Hg^{2+} adsorbed was calculated as described in Section 2.2. In addition, to evaluate the Hg^{2+} adsorption mechanism, the concentration of potassium ions released from FA48 in the adsorption isotherm experiment was measured using an iCAP-7600 Duo (Thermo Fisher Scientific Inc., Osaka, Japan).

2.4. Effect of Coexistences on the Adsorption of Hg^{2+}

In order to evaluate the selectivity of Hg^{2+} adsorption, FA48 (0.01 g) was added to the binary solution of 50 mL. The two components were Hg^{2+} and Na^{+}, Mg^{2+}, K^{+}, Ca^{2+}, Ni^{2+}, Cu^{2+}, Zn^{2+}, Sr^{2+}, or Cd^{2+}, and Hg^{2+} or individual cation concentration was 10 mg/L in a binary solution. The sample solution was shaken at 100 rpm at 25 °C for 24 h and filtered through a 0.45 μm membrane filter. The concentration of each metal was measured using an iCAP-7600 Duo. The amount adsorbed was calculated by comparing the levels before and after adsorption.

2.5. Adsorption/Desorption of Hg^{2+} Using Sodium Hydroxide Solution

To evaluate the recycling of FA48 in Hg^{2+} adsorption/desorption, FA48 (0.15 g) was added to a 150 mL Hg^{2+} solution at 250 mg/L. The suspension was shaken at 100 rpm, 25 °C for 24 h, and filtered through a 0.45 µm membrane filter. The concentration of Hg^{2+} was measured using an iCAP-7600 Duo. The amount of Hg^{2+} adsorbed was calculated as described in Section 2.2. After adsorption, FA48 was collected, dried, and used for the desorption experiment. The collected FA48 (0.05 g) was added to 50 mL sodium hydroxide solution at 10, 100, 1000 mmol/L. The suspension was shaken at 100 rpm, 25 °C for 24 h, and filtered through a 0.45 µm membrane filter. The concentration of Hg^{2+} released from FA48 was also measured using an iCAP-7600 Duo. The amount of Hg^{2+} desorbed was calculated using the levels before and after desorption. All results in this study are expressed as mean ± standard error (n = 2–3, Sections 2.2–2.5). In addition, each Figure was prepared using Microsoft Excel.

3. Results and Discussion

3.1. Properties of Potassium-Type Zeolite

Zeolites are characterized by physicochemical properties, such as specific surface area, pore volume, and CEC (Table 1). These characteristics are related to the parameters of hydrothermal treatment, such as heat temperature, pressure, solution alkalinity, activation solution to CFA ratio, and formation process [18]. In this study, six types of potassium-type zeolites were prepared using the above-mentioned method [28]. In addition, our previous study reported the physicochemical properties of potassium-type zeolites in detail [28]. The XRD patterns indicate that CFA was mainly composed of mullite and quartz. The XRD patterns of FA1, FA3, FA6 and FA12 were similar to those of CFA under our experimental conditions. Zeolite F appeared in FA24 and FA48 structures. We observed changes in the surface of FA series with the treatment time. Aluminosilicate gels were clearly produced on FA24 and FA48 surfaces. These processes were in the following order: Al and Si dissolution, geopolymer formation, crystalline structure nucleation, finally zeolite crystal growth [18]. The CEC of FA48 (8.98–11.77 mmol/g) was the highest compared to other FA series. This value of FA48 was 26–69 times higher than that of CFA. The pH_{pzc} of FA was 9.8, and that of FA24 and FA48 were 10.4. Finally, specific surface area and pore volume ($d \leqq 20$ Å) of FA48 (47.3 m^2/g and 10 Å) was 34 and 100 times higher than CFA. Additionally, the value of FA48 (potassium-type zeolite) was greater than that of sodium-type zeolite [32]. Thus, these results indicate that potassium-type zeolite (FA48) can be prepared from coal fly ash by conventional hydrothermal treatment using potassium hydroxide.

Table 1. Characteristics of the zeolite samples.

Adsorbents		CFA	FA1	FA3	FA6	FA12	FA24	FA48
CEC ($mmol\ g^{-1}$)	pH 5	0.34	1.98	1.17	1.63	2.27	7.90	8.98
	pH 10	0.19	0.65	1.55	2.09	3.46	11.17	11.17
pH_{pzc}		9.8	9.3	9.3	9.5	9.7	10.4	10.4
Specific surface area (m^2/g)		1.4	15.1	31.5	53.3	54.5	50.3	47.3
Pore volume (µL/g)	$d \leqq 20$ (Å)	0.1	0.9	0	0.5	0.2	10.0	10.0
	$20 < d \leqq 500$ (Å)	2.0	41.9	97.4	161.5	185.0	105.0	99.0
	Total	2.2	63.0	139.0	221.0	220.0	151.0	131.0
Mean pore diameter (Å)		57.0	167.2	176.7	165.9	161.6	120.1	110.7

3.2. Adsorption of Hg^{2+}

Figure 1 shows the quantity of Hg^{2+} adsorbed by the FA series. The adsorbed Hg^{2+} was in the order CFA, FA1 (0–0.48 mg/g) < FA3 (2.2 mg/g) < FA6 (3.5 mg/g) < FA12 (4.0 mg/g) < FA24 (7.5 mg/g) < FA48 (11.6 mg/g) in the current experiment conditions. The adsorption capability of Hg^{2+} using the FA series depended on the duration of the hydrothermal activation treatment using potassium hydroxide solution. Next, we evaluated

the relationship between the adsorption capacity of Hg^{2+} and the physicochemical properties of the FA series. As a result, the positive correlation coefficient between the quantity of Hg^{2+} adsorbed and CEC, specific surface area, and pore volume ($d \leqq 20$ Å) were 0.928, 0.659, and 0.882, respectively. These results indicate that CEC and pore volume strongly affect the adsorption of Hg^{2+} from aqueous solutions. Additionally, in this study, FA48 was selected to evaluate the adsorption capability for Hg^{2+} removal from aqueous solutions.

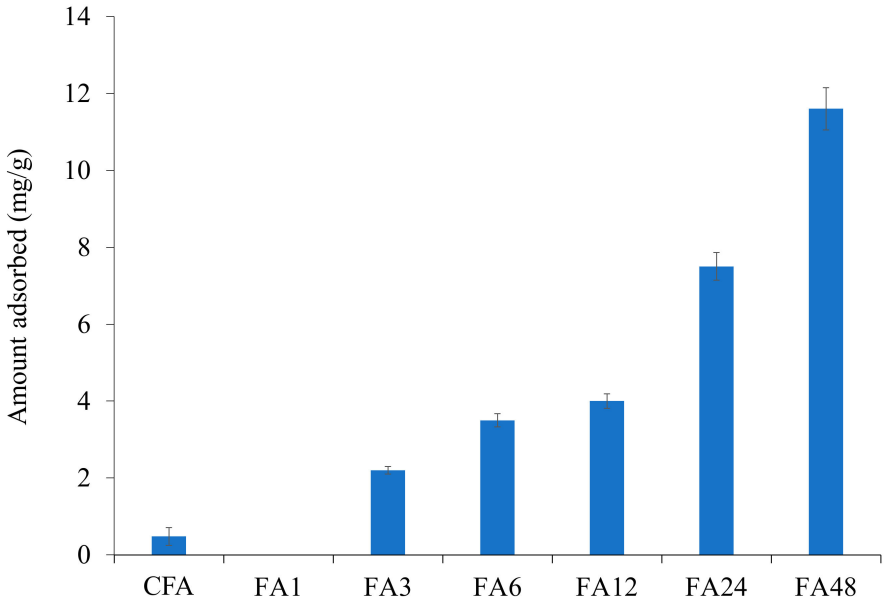

Figure 1. Quantity of Hg^{2+} adsorbed onto FA series. Initial concentration: 50 mg/L, sample volume: 50 mL, adsorbent: 0.01 g, temperature: 25 °C, contact time: 24 h, agitation speed: 100 rpm, pH: 3.0.

A comparison of the Hg^{2+} adsorption capability of FA48 with that of the other adsorbents is listed in Table 2 [24,26,32–35]. FA48 exhibited potential in Hg^{2+} adsorption from aqueous solutions compared to other reported adsorbents (except for coal gangue and multifunctional mesoporous material).

Table 2. Comparison of Hg^{2+} adsorption capacity of FA48 with other reported adsorbents.

Adsorbents	Adsorption Capability (mg/g)	pH	Temp. (°C)	Initial Concentration (mg/L)	Contact Time (h)	Adsorbent (g/L)	Ref.
Coal gangue	20.0	5.5	25	3.5	0.17	2.5	33
Microwave-assisted alkali-modified fly ash	2.7	-	25	~50	1.5	10	24
Raw coal ash zeolite sample	0.44	2.5	r.t.	10	24	1	26
Multifunctional mesoporous material	21.05	Not provided	25	Not provided	2	Not provided	34
Thiol-functionalized mesoporous silica-coated magnetite nanoparticle	9.5	6.0	22.5	8	15	8.0×10^{-5}	35
Sodium-type zeolite prepared from fly ash	7.5	3.0	25	10	24	0.2	32
FA48	11.6	3.0	25	50	24	0.2	This study

3.3. Adsorption Isotherms of Hg^{2+}

Figure 2 shows the adsorption isotherms of Hg^{2+} using FA48 at different temperatures. The quantity of Hg^{2+} adsorbed using FA48 did not significantly vary with different

temperatures. Therefore, in this study, the adsorption temperature did not strongly affect the adsorption capability of FA48.

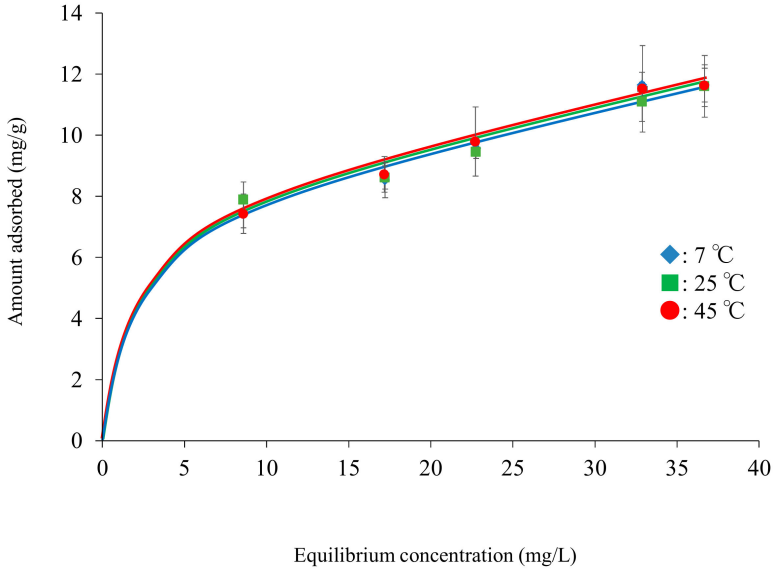

Figure 2. Adsorption isotherms of Hg^{2+} at different temperatures. Initial concentration: 10, 20, 30, 40, and 50 mg/L, sample volume: 50 mL, adsorbent: 0.01 g, temperature: 7, 25, and 45 °C, contact time: 24 h, agitation speed: 100 rpm.

Additionally, to investigate the adsorption properties and interactions, the adsorption isotherm data were evaluated using the Freundlich and Langmuir isotherm models. The Freundlich isotherm model was applied to multilayer adsorption, while the Langmuir isotherm model showed monolayer adsorption at specific homogenous sites [24].

The Freundlich isotherm model can be represented as follows [36]:

$$\log q = \frac{1}{n} \log C + \log K_F \tag{2}$$

where q is the quantity of Hg^{2+} adsorbed (mg/g), K_F and $1/n$ are the Freundlich isotherm constants, C is the equilibrium concentration (mg/L). In general, the adsorption reaction in the aqueous phase fits this model. In the Freundlich isotherm model, the isotherm curve depends on the value of n. In particular, when the value of $1/n$ is 0.1–0.5, adsorption occurs easily, when $1/n$ is over 2, it is difficult to adsorb [37].

The Langmuir isotherm model can be represented as follows [38]:

$$\frac{1}{q} = \frac{1}{q_{\max}} + \left(\frac{1}{K_L q_{\max}}\right)\left(\frac{1}{C}\right) \tag{3}$$

where K_L is the Langmuir isotherm constant (L/mg) and $q_{\max}$ is the maximum quantity adsorbed (mg/g). The Langmuir isotherm model is a theoretical model that can explain monolayer adsorption onto homogenous surfaces. In addition, this model considers adsorption sites.

Table 3 shows the Freundlich and Langmuir model constants for the adsorption of Hg^{2+} using FA48. The obtained data fitted both models (correlation coefficient of the Freundlich and Langmuir equations were $\geq$ 0.960 and $\geq$ 0.904, respectively). The maximum quantity adsorbed at 7 to 45 °C was not significantly different in this study, which is supported by the adsorption isotherm data in Figure 2. In addition, the value of $1/n$ was from 0.27 to 0.33 in this study. Therefore, the adsorption of Hg^{2+} using FA48 from aqueous solutions is more favorable.

Table 3. Freundlich model and Langmuir model constants for the adsorption of Hg^{2+}.

Sample	Temp. (°C)	Langmuir Constants			Freundlich Constants		
		q_{max} (mg/g)	K_L (L/mg)	r	$\log K_F$	$1/n$	r
FA48	7	13.25	0.14	0.942	0.55	0.33	0.977
	25	12.27	0.19	0.904	0.63	0.27	0.960
	45	13.35	0.14	0.962	0.56	0.32	0.989

Finally, adsorption properties were evaluated using Sips equation (Equation (4)). The Sips model was derived from the Langmuir and Freundlich equations. This model predicts the heterogeneous adsorption system and overcoming the drawback associated with Freundlich model [39]. The Sips equation was expressed as follows:

$$\frac{1}{q_e} = \frac{1}{Q_{max} K_S} \left(\frac{1}{C_e}\right)^{1/n} + \frac{1}{Q_{max}} \quad (4)$$

where K_S is the Sips equilibrium constant (L/mg), Q_{max} is the maximum quantity adsorbed (mg/g). n is the Sips model exponent, which can be employed to describe the system's heterogeneity. If the value of n is equal to 1, this equation will become a Langmuir equation. It means a homogeneous adsorption process [40,41].

Table 4 shows the Sips model constants for the adsorption of Hg^{2+}. The value of correlation coefficient of Sips equation was from 0.841 to 0.959 under our experimental conditions. The values of Q_{max} at 7–45 °C was not significantly changed, which is similar trends to the adsorption isotherm data (Figure 2). In addition, the heterogeneous factor values (n = 0.4–1.1) indicate that heterogeneous adsorption process is related to the adsorption mechanism of Hg^{2+} using FA48.

Table 4. Sips model constants for the adsorption of Hg^{2+}.

Sample	Temp. (°C)	K_S (L/mg)	Q_{max} (mg/g)	n	r
FA48	7	0.84	11.6	1.1	0.959
	25	19.4	11.6	0.6	0.858
	45	4.1×10^2	11.6	0.4	0.841

Moreover, to evaluate the adsorption mechanism of Hg^{2+} using FA48, more detailed investigations were conducted in this study (Figure 3). First, the relationship between the quantity of Hg^{2+} adsorbed and the quantity of K^+ released from FA48 was evaluated in this study. As a result, the correlation coefficient value (r) was positive at 0.946, indicating that ion exchange with K^+ in the interlayer of FA48 was one of the mechanisms of Hg^{2+} adsorption from aqueous media. As mentioned in Section 3.2, the positive correlation coefficient between the quantity of Hg^{2+} adsorbed and the value of CEC was 0.928. These trends were similar to those reported in previous studies [28,32]. Additionally, the X-ray photoelectron spectroscopy analysis was conducted in this study. The peak intensity of Hg(5p) at 67 eV was newly detected after the adsorption of Hg^{2+}, indicating that Hg^{2+} was present on the FA48 surface after adsorption, and was not detected before adsorption. Generally, Hg(4f) peaks at 101 and 105 eV were detected after adsorption. However, Si(2p) and Hg(4f) peaks overlapped in this study. Therefore, it was difficult to elucidate and/or detect these peaks in our experiments.

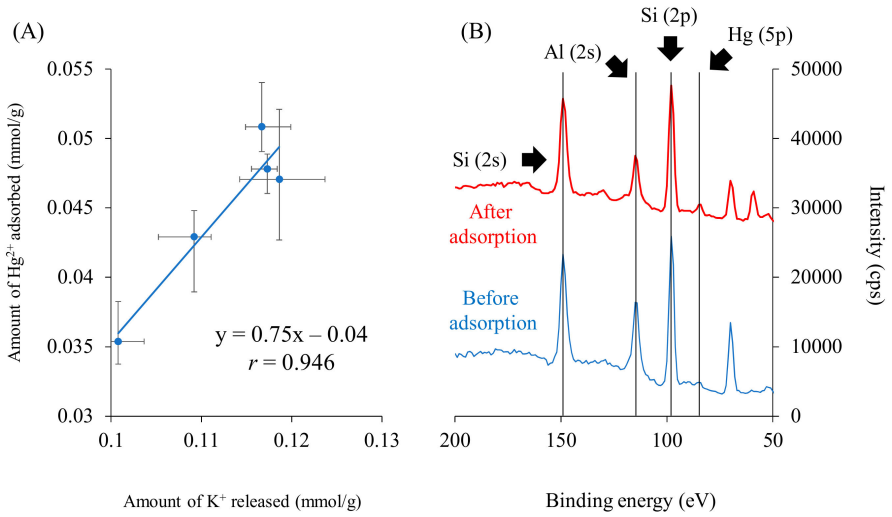

Figure 3. Relationship between the quantity of Hg^{2+} adsorbed and K^+ released (**A**) and the X-ray photoelectron spectroscopy analysis before and after adsorption of Hg^{2+} (**B**). Initial concentration: 50 mg/L, sample volume: 50 mL, adsorbent: 0.01 g, temperature: 25 °C, contact time: 24 h, agitation speed: 100 rpm.

3.4. Effect of Solution pH on the Adsorption of Hg^{2+}

In aqueous media, pH is one of the most important parameters for heavy metal removal. Thus, the solution pH strongly and directly affects the degree of metal ionization and/or metal binding on the adsorbent surface sites [42]. In this study, the quantity of Hg^{2+} adsorbed onto FA24 increased with an increase in the solution pH from 2 to 5, and decreased with further increase in pH of 5 to 7 (Figure 4). First, when the solution pH is below 3, Hg^{2+} is the dominant species; when the solution pH is over 5, $Hg(OH)_2$ is the dominant species [43,44]. In addition, $Hg(OH)^+$ exists (1–13% of the total mercury Hg^{2+}) when the solution pH is between 2 and 6. Previous studies have reported that there are several stable Hg^{2+} products related to either the equilibrium hydrolysis (such as $Hg(OH)_3^-$, $Hg(OH)_2$, $Hg(OH)^+$) or to the complexation equilibrium with chloride (such as $HgCl_4^{2-}$, $HgCl_3^-$, $HgCl_2$, $HgCl^+$). Moreover, mixed species such as Hg(OH)Cl exist in aqueous media [44]. In an acidic solution (pH 2), the FA48 surface is protonated and the electrostatic repulsion between the FA48 surface (positive charge) and Hg^{2+} species (positive charge) such as $Hg(OH)^+$ and $HgCl^+$ easily occurred, resulting in low Hg adsorption. Additionally, the pH_{pzc} value of FA48 was 10.4 in this study, which supports the availability of positive charge on the FA48 surface and the low adsorption of Hg^{2+} from aqueous media. Next, similar to pH 2, at pH 5, the quantities of Hg^{2+} species such as $Hg(OH)^+$ and $HgCl^+$ decreased. Conversely, $HgCl_3^-$ species increased in aqueous media. Therefore, the quantity of Hg^{2+} adsorbed increased because of the electrostatic interaction between the FA48 surface (positive charge) and Hg^{2+} species such as $HgCl_3^-$ (negative charge). Finally, when the solution pH was over 7, the quantity of $Hg(OH)_2$ increased, and the hydroxyl ion (OH^-) also increased in the sample solution media [6,43]. Therefore, FA48 showed a low adsorption capability for Hg^{2+} under alkaline conditions.

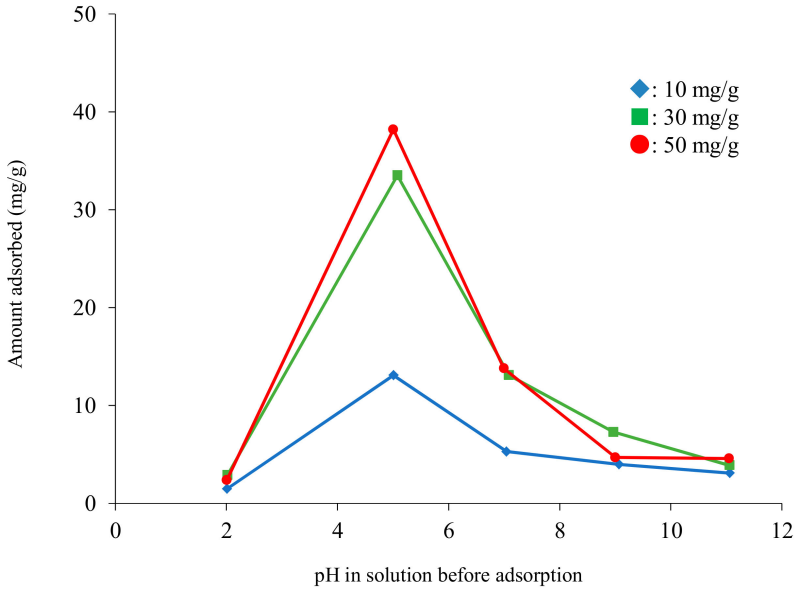

Figure 4. Effect of pH on the adsorption of Hg^{2+} onto FA48. Initial concentration: 10, 30, and 50 mg/L, sample volume: 50 mL, adsorbent: 0.01 g, temperature: 25 °C, contact time: 24 h, 100 rpm.

3.5. Effect of Contact Time on the Adsorption of Hg^{2+}

To investigate the effect of contact time on the removal of Hg^{2+} from aqueous media using FA48, the duration was varied from 0.5 to 48 h (Figure 5). Rapid adsorption was observed within 0.5 h from the start of the adsorption process, following which the rate of adsorption of Hg^{2+} fluctuated with increase in adsorption time. Finally, adsorption equilibrium was achieved at approximately 3 h under our experimental conditions. In this study, the adsorption might be mainly attributed to two factors: the interaction between Hg^{2+} and active adsorption sites, such as specific surface area and pore volume (mentioned in Section 3.2), and ion exchange with K^+ in the interlayer of FA48 (mentioned in Section 3.3).

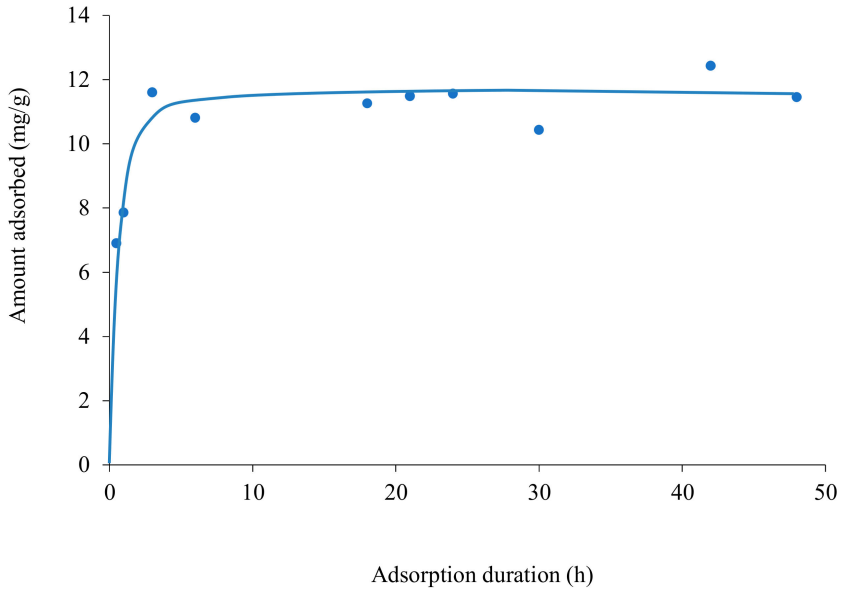

Figure 5. Effect of contact time on the adsorption of Hg^{2+} onto FA48. Initial concentration: 50 mg/L, sample volume: 50 mL, adsorbent: 0.01 g, temperature: 25 °C, contact time: 0.5, 1, 3, 6, 12, 21, 24, 30, 42, and 48 h, agitation speed: 100 rpm.

In addition, to evaluate the kinetic adsorption mechanism of Hg^{2+} using FA48, pseudo-first-order and pseudo-second-order models were selected to interpret the kinetics data using Equations (5) and (6) [36,38].

$$\ln(q_{e,exp} - q_t) = \ln q_{e,cal} - k_1 t \quad (5)$$

$$\frac{t}{q_t} = \frac{t}{{q_{e,cal}}^2} + \frac{1}{k_2 \times {q_{e,cal}}^2} \quad (6)$$

where $q_{e,exp}$ and q_t are the quantities of Hg^{2+} adsorbed at equilibrium and at time t (mg/g), respectively, $q_{e,cal}$ is the quantity of Hg^{2+} adsorbed in the calculation (mg/g), k_1 (1/h) and k_2 (g/mg/h) are the rate constants of the pseudo-first-order and pseudo-second-order models, respectively. The calculated results are shown in Table 5.

Table 5. Kinetic parameters for the adsorption of Hg^{2+} using FA48.

Adsorbents	$q_{e,exp}$	Pseudo-First-Order Model			Pseudo-Second-Order Model		
		k_1 (1/h)	$q_{e,cal}$ (mg/g)	r	k_2 (g/mg/h)	$q_{e,cal}$ (mg/g)	r
FA48	12.42	0.02	2.34	0.515	0.085	11.7	0.996

From Table 5, it is evident that the correlation coefficient (r) in the pseudo-second-order model (0.996) was significantly higher than the pseudo-first-order model (0.515), indicating that the pseudo-second-order model is more suitable for describing the adsorption kinetics of Hg^{2+} in this study. Additionally, the value of $q_{e,exp}$ was closest to the value of $q_{e,cal}$ of the pseudo-second-order model than that of the pseudo-first-order model. In addition, it is strongly suggested that the adsorption of Hg^{2+} onto FA48 is because of chemisorption, as assumed by this model [45,46].

In addition, the Elovich model (Equation (7)) was also used to describe adsorption kinetic in this study. This model describes activated adsorption, and predicts an energetically heterogeneous solid surface of adsorbent which means adsorption kinetics is not affected by interaction between the adsorbent particles [26].

$$q_t = 1/\beta \ln(\alpha\beta) + 1/\beta \ln t \quad (7)$$

where q_t is the quantity of Hg^{2+} adsorbed at time t (mg/g), α is the initial adsorption rate (mg/g/h), β is the related to the extent of surface coverage and activation energy for chemisorption (g/mg).

From the result, the value of α, β, and r (correlation coefficient) was 8.4×10^3 mg/g/h, 1.1 g/mg, and 0.888, respectively. The Elovich equation is suitable to describe adsorption behavior of Hg^{2+} using FA48 that relates to the nature of chemical sorption under our experimental conditions [47].

3.6. Selectivity for Hg^{2+} Removal from Binary Solution System

Considering the field application of FA48, the selectivity for Hg^{2+} adsorption is one of the critical parameters in this study. Therefore, the effect of coexisting ions on the adsorption capability of Hg^{2+} is shown in Table 6. In our study, Na^+, Mg^{2+}, K^+, Ca^{2+}, Ni^{2+}, Cu^{2+}, Zn^{2+}, Sr^{2+}, and Cd^{2+} were used as the components of the binary solution system, as these ions are ubiquitous in the water environment [48,49]. In this study, the removal percentage of Hg^{2+} using FA48 in a single solution system was approximately 14.0% whereas, the removal of Hg^{2+} in the binary solution system was over 11.4% (except for Na^+ and K^+), and the removal of other cations was significantly lower. A similar trend was reported in a previous study [6]. In addition, previous studies reported that the radius of the hydrated ion and/or the electronegativity of the adsorbate (Hg^{2+} in this study) strongly and directly influenced the adsorption capability in aqueous media [48,49].

Therefore, similar phenomena were observed under our experimental conditions. Finally, our results show that FA48 is useful for the selective removal of Hg^{2+} from aqueous media. Moreover, the Minamata Convention on Mercury was adopted by the Intergovernmental Negotiating Committee in 2017. Therefore, the development of removal techniques for Hg^{2+} in wastewater from anthropogenic activities such as the steel industry is very important for establishing a sustainable society. Thus, FA48 could be applied for wastewater purification including Hg^{2+} such as the steel industry.

Table 6. Adsorption capacity of Hg^{2+} in binary solution system.

Components in Binary Solution	Removal Percentage of Hg^{2+} (%)	Removal of Other Cations (%)
$Hg^{2+} + Na^{+}$	4.6	0
$Hg^{2+} + Mg^{2+}$	11.4	0
$Hg^{2+} + K^{+}$	5.1	0
$Hg^{2+} + Ca^{2+}$	11.9	0
$Hg^{2+} + Ni^{+}$	16.2	0.1
$Hg^{2+} + Cu^{2+}$	12.9	2.4
$Hg^{2+} + Zn^{2+}$	16.0	1.3
$Hg^{2+} + Sr^{2+}$	15.9	0
$Hg^{2+} + Cd^{2+}$	14.4	1.8

3.7. Adsorption/Desorption Capability of Hg^{2+} Using FA48

Finally, the adsorption/desorption capability of Hg^{2+} using FA48 was demonstrated in this study (Figure 6). The quantity of Hg^{2+} desorbed increased with increasing concentration of sodium hydroxide solution from 10 to 1000 mmol/L (the quantity of Hg^{2+} adsorbed was approximately 40 mg/g). The desorption percentages using 10, 100, and 1000 mmol/L sodium hydroxide solutions were 37.5%, 41.6%, and 68.3%, respectively. Therefore, adsorbed Hg^{2+} onto FA48 could be easily desorbed using a sodium hydroxide solution under our experimental conditions. Further investigations are needed to elucidate the application of FA48 in these fields.

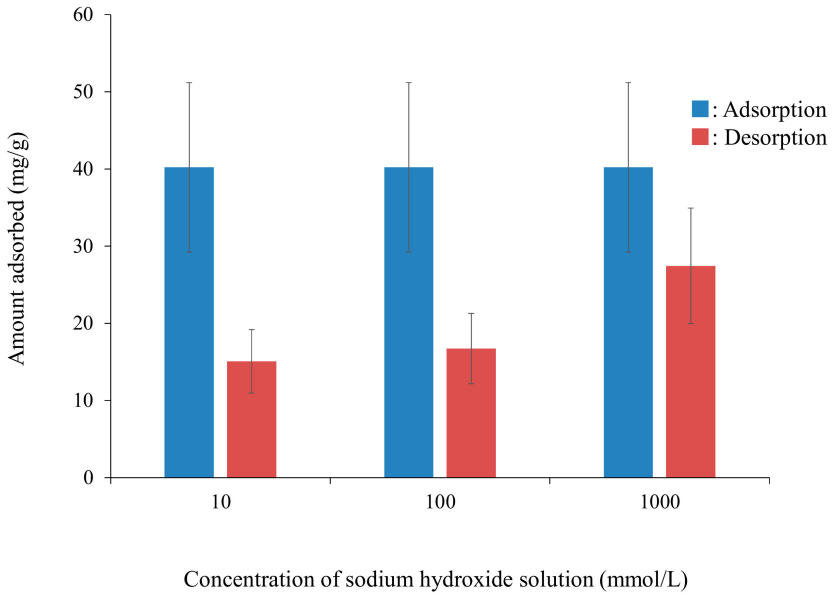

Figure 6. Adsorption/Desorption capability of Hg^{2+} using FA48. Adsorption condition; initial concentration: 250 mg/L, sample volume: 150 mL, adsorbent: 0.15 g, temperature: 25 °C, contact time: 24 h, agitation speed: 100 rpm, Desorption condition; initial concentration: 10, 100, and 1000 mmol/L, sample volume: 50 mL, adsorbent: 0.05 g, temperature: 25 °C, contact time: 24 h, agitation speed: 100 rpm.

4. Conclusions

Six types of potassium zeolites (FA1, FA3, FA6, FA12, FA24, FA48) were synthesized by hydrothermal treatment using a potassium hydroxide solution. The values of CEC, specific surface area, and pore volume ($d \leqq 20$ Å) of FA48 were 26–29, 34, and 100 times higher than that of CFA, indicating that FA48 has a high potential for the removal of Hg^{2+} from aqueous media. The quantity of Hg^{2+} was in the order CFA and FA1 (0–0.48 mg/g) < FA3 (2.2 mg/g) < FA6 (3.5 mg/g) < FA12 (4.0 mg/g) < FA24 (7.5 mg/g) < FA48 (11.6 mg/g) under our experiment conditions. These adsorption behaviors were affected by the CEC and/or pore volume ($d \leq 20$ Å). In addition, the effects of pH, temperature, contact time, and coexistences on the adsorption of Hg^{2+} using FA48 were demonstrated. The optimal pH was approximately 5.0. The adsorption isotherm data or kinetics data were described by the Freundlich and Langmuir models or the pseudo-second-order model, respectively. Moreover, one of the adsorption mechanisms determined was the ion exchange with K^+ in the interlayer of FA48 (correlation coefficient = 0.946). FA48 showed selectivity for the adsorption of Hg^{2+} from a binary solution system containing Na^+, Mg^{2+}, K^+, Ca^{2+}, Ni^{2+}, Cu^{2+}, Zn^{2+}, Sr^{2+}, or Cd^{2+}. Finally, adsorbed Hg^{2+} onto FA48 was easily desorbed using a sodium hydroxide solution. It is evident that FA48 is a useful adsorbent for Hg^{2+} removal from aqueous media. These techniques may potentially aid in mitigating heavy metal pollution and thus contribute to the establishment of a sustainable society.

Author Contributions: Conceptualization, F.O. and N.K.; investigation, Y.K., C.S., and T.N.; writing—original draft preparation, Y.K. and F.O.; writing—review and editing, F.O. and N.K.; project administration, N.K. All authors have read and agreed to the published version of the manuscript.

Funding: This research received no external funding.

Institutional Review Board Statement: Not applicable.

Informed Consent Statement: Not applicable.

Data Availability Statement: Not applicable.

Conflicts of Interest: The authors declare no conflict of interest.

References

1. Sustainable Development Goals, Knowledge Platform. Available online: https://sustainabledevelopment.un.org/sdgs (accessed on 10 June 2020).
2. Kragovic, M.; Dakovic, A.; Markovic, M.; Krstic, J.; Gatta, G.D.; Rotiroti, N. Characterization of lead sorption by the natural and Fe(III)-modified zeolite. *Appl. Surf. Sci.* **2013**, *283*, 764–774. [CrossRef]
3. Hamidpour, M.; Kalbasib, M.; Afyunib, M.; Shariatmadarib, H.; Holmic, P.E.; Hansenc, H.C.B. Sorption hysteresis of Cd(II) and Pb(II) on natural zeolite and bentonite. *J. Hazard. Mater.* **2010**, *181*, 686–691. [CrossRef] [PubMed]
4. Volesky, B. *Biosorption of Heavy Metals*, 4th ed.; CRC Press: Boca Raton, FL, USA, 1990.
5. Abraham, J.; Dowling, K.; Florentine, S. Assessment of potentially toxic metal contamination in the soils of a legacy mine site in Central Victoria, Australia. *Chemosphere* **2018**, *192*, 122–132. [CrossRef] [PubMed]
6. Fu, Y.; Jiang, J.; Chen, Z.; Ying, S.; Wang, J.; Hu, J. Rapid and selective removal of Hg(II) ions and high catalytic performance of the spent adsorbent based on functionalized mesoporous silica/poly (m-aminothiophenol) nanocomposite. *J. Mol. Liq.* **2019**, *286*, 110746. [CrossRef]
7. Wang, J.; Feng, X.; Anderson, C.W.N.; Xing, Y.; Shang, L. Remediation of mercury contaminated sites—A review. *J. Hazard. Mater.* **2012**, *221*, 1–18. [CrossRef]
8. World Health Organization. *Guidelines for Drinking-Water Quality, First Addendum to Volume 1, Recommendations*; WHO Press: Geneva, Switzerland, 2006.
9. IARC Monographs on the Identification of Carcinogenic Hazards to Human. Available online: https://monographs.iarc.fr/list-of-classifications (accessed on 10 June 2020).
10. Awual, M.R.; Hasan, M.M.; Eldesoky, G.E.; Khaleque, M.A.; Rahman, M.M.; Naushad, M. Facile mercury detection and removal from aqueous media involving ligand impregnated conjugate nanomaterials. *Chem. Eng. J.* **2016**, *290*, 243–251. [CrossRef]
11. Venkateswarlu, S.; Yoon, M. Surfactant-free green synthesis of Fe_3O_4 nanoparticles capped with 3,4-dihydroxyphenethylcarbamodithioate: Stable recyclable magnetic nanoparticles for rapid and efficient removal of Hg(II) ions from water. *Dalton Trans.* **2015**, *44*, 18427–18437. [CrossRef]

12. Bukhari, S.S.; Behin, J.; Kazemian, H.; Rohani, S. Conversion of coal fly ash to zeolite utilizing microwave and ultrasound energies: A review. *Fuel* **2015**, *140*, 250–266. [CrossRef]
13. Czarna-Juszkiewicz, D.; Kunecki, P.; Panek, R.; Madej, J.; Wdowin, M. Impact of fly ash fraction on the zeolitization process. *Materials* **2020**, *13*, 1035. [CrossRef]
14. Yao, Z.T.; Ji, X.S.; Sarker, P.K.; Tang, J.H.; Ge, L.Q.; Xia, M.S.; Xi, Y.Q. A comprehensive review on the applications of coal fly ash. *Earth Sci. Rev.* **2015**, *141*, 105–121. [CrossRef]
15. Franus, W.; Wdowin, M.; Franus, M. Synthesis and characterization of zeolites prepared from industrial fly ash. *Environ. Monit. Assess.* **2014**, *186*, 5721–5729. [CrossRef]
16. Blissett, R.S.; Rowson, N.A. A review of the multi-component utilization of coal fly ash. *Fuel* **2012**, *97*, 1–23. [CrossRef]
17. Flores, C.G.; Schneider, H.; Marcillio, N.R.; Ferret, L.; Oliveira, J.C.P. Potassic zeolites from Brazilian coal ash for use as a fertilizer in agriculture. *Waste Manag.* **2017**, *70*, 263–271. [CrossRef]
18. Belviso, C. State-of-the-art applications of fly ash from coal and biomass: A focus on zeolite synthesis processes and issues. *Prog. Energy Comb. Sci.* **2018**, *65*, 109–135. [CrossRef]
19. Medina, A.; Gamero, P.; Almanza, J.M.; Vargas, A.; Montoya, A.; Vargas, G.; Izquierdo, M. Fly ash from a Mexican mineral coal. II. Source of W zeolite and its effectiveness in arsenic (V) adsorption. *J. Hazard. Mater.* **2010**, *181*, 91–104. [CrossRef]
20. Scott, J.; Guang, D.; Naeramitmarnsuk, K.; Thabuot, M.; Amal, R. Zeolite synthesis from coal fly ash for the removal of lead ions from aqueous solution. *J. Chem. Technol. Biotechnol.* **2001**, *77*, 63–69. [CrossRef]
21. Rayalu, S.; Meshram, S.U.; Hasan, M.Z. Highly crystalline faujasitic zeolites from fly ash. *J. Hazard. Mater.* **2000**, *77*, 123–131. [CrossRef]
22. Rios, C.A.; Williams, C.D.; Roberts, C.L. Removal of heavy metals from acid mine drainage (AMD) using coal fly ash, natural clinker and synthetic zeolites. *J. Hazard. Mater.* **2008**, *156*, 23–35. [CrossRef]
23. Tauanov, Z.; Tsakiridis, P.E.; Mikhalovsky, S.V.; Inglezakis, V.J. Synthetic coal fly ash-derived zeolites doped with silver nanoparticles for mercury(II) removal from water. *J. Environ. Manag.* **2018**, *224*, 164–171. [CrossRef]
24. Ma, L.; Han, L.; Chen, S.; Hu, J.; Chang, L.; Bao, W.; Wang, J. Rapid synthesis of magnetic zeolite materials from fly ash and iron-containing wastes using supercritical water for elemental mercury removal from flue gas. *Fuel Proc. Technol.* **2019**, *189*, 39–48. [CrossRef]
25. Qi, L.; Teng, F.; Deng, X.; Zhang, Y.; Zhong, X. Experimental study on adsorption of Hg(II) with microwave-assisted alkali-modified fly ash. *Powder Technol.* **2019**, *341*, 153–158. [CrossRef]
26. Attari, M.; Bukhar, S.S.; Kazemian, H.; Rohani, S. A low-cost adsorbent from coal fly ash for mercury removal from industrial wastewater. *J. Environ. Chem. Eng.* **2017**, *5*, 391–399. [CrossRef]
27. Murayama, N.; Ymamamoto, H.; Shibata, J. Mechansim of zeolite synthesis from coal fly ash by alkali hydrothermal reaction. *Int. J. Miner. Process.* **2002**, *64*, 1–17. [CrossRef]
28. Kobayashi, Y.; Ogata, F.; Saenjum, C.; Nakamura, T.; Kawasaki, N. Removal of Pb^{2+} from aqueous solutions using K-type zeolite synthesized from coal fly ash. *Water* **2020**, *12*, 2375. [CrossRef]
29. Zhou, Q.; Duan, Y.; Zhu, C.; Zhang, J.; She, M.; Wei, H.; Hong, Y. Adsorption equilibrium, kinetics and mechanism studies of mercury on coal-fired fly ash. *Korean J. Chem. Eng.* **2015**, *32*, 1405–1413. [CrossRef]
30. Okada, Y. Synthesis of zeolite using fly ash on cloased system. *Nihon Dojyou Hiryo Gakkaishi* **1991**, *62*, 1–6.
31. Faria, P.C.C.; Orfao, J.J.M.; Pereira, M.F.R. Adsorption of anionic and cationic dyes on activated carbons with different surface chemistries. *Water Res.* **2004**, *38*, 2043–2052. [CrossRef]
32. Kobayashi, Y.; Ogata, F.; Nakamura, T.; Kawasaki, N. Synthesis of novel zeolites produced from fly ash hydrothermal treatment in alkaline solution and its evaluation as an adsorbent for heavy metal. *J. Environ. Chem. Eng.* **2020**, *8*, 103687. [CrossRef]
33. Shang, Z.; Zhang, L.; Zhao, X.; Liu, S.; Li, D. Removal of Pb(II), Cd(II) and Hg(II) from aqueous solution by mercapto-modified coal gangue. *J. Environ. Manag.* **2019**, *231*, 391–396. [CrossRef]
34. Wang, C.; Tao, S.; Wei, W.; Meng, C.; Liu, F.; Han, M. Multifunctional mesoporous material for detection, adsorption and removal of Hg^{2+} in aqueous solution. *J. Mater. Chem.* **2010**, *20*, 4635–4641. [CrossRef]
35. Hakami, O.; Zhang, Y.; Banks, C. Thiol-functionalized mesoporous silica-coated magnetite nanoparticles for high efficiency removal and recovery of Hg from water. *Water Res.* **2012**, *46*, 3913–3922. [CrossRef]
36. Lagergren, S. Zur theorie der sogenannten adsorption geloster stoffie. *K. Sven. Vetensk. Handl.* **1898**, *24*, 1–39.
37. Abe, I.; Hayashi, K.; Kitagawa, M. Studies on the adsorption of surfactants on activated carbons. I. Adsorption of nonionic surfactants. *Yukagaku* **1976**, *25*, 145–150.
38. Ho, Y.S.; McKay, G. Pseudo-second order model for sorption process. *Process Biochem.* **1999**, *34*, 451–465. [CrossRef]
39. Kumar, V. Adsorption kinetics and isotherms for the removal of rhodamine B dye and Pb^{2+} ions from aqueous solutions by a hybrid ion-exchanger. *Arab. J. Chem.* **2019**, *12*, 316–329.
40. Foo, K.Y.; Hameed, B.H. Insights into the modeling of adsorption isotherms systems. *Chem. Eng. J.* **2010**, *156*, 2–10. [CrossRef]
41. Kumara, N.T.R.N.; Hamdan, N.; Peter, M.I.; Tennakoon, K.T.; Ekanayake, P. Equilibrium isotherm studies of adsorption of pigments extracted from Kuduk-kuduk (*Melastoma malabathricum* L.) pulp onto TiO_2 nanoparticles. *J. Chem.* **2014**, *2014*, 468975. [CrossRef]
42. Liu, U.; Li, Q.; Cao, X.; Wang, Y.; Jiang, X.; Li, M.; Hua, M.; Zhang, Z. Removal of uranium(VI) from aqueous solutions by CMK-3 and its polymer composite. *Chem. Eng.* **2013**, *285*, 258–266. [CrossRef]

43. Zhang, F.S.; Nriagu, J.O.; Itoh, H. Mercury removal from water using activated carbons derived from organic sewage sludge. *Water Res.* **2005**, *39*, 389–395. [CrossRef]
44. Arisa, F.E.; Beneduci, A.; Chidichimo, F.; Furia, E.; Straface, S. Study of the adsorption of mercury (II) on lignocellulosic materials under static and dynamic conditions. *Chemosphere* **2017**, *180*, 11–23.
45. Boparai, H.K.; Joseph, M.; O'Carroll, D.M. Kinetics and thermodynamics of cadmium ion removal ion removal by adsorption onto nano zerovalent iron particles. *J. Hazard. Mater.* **2011**, *186*, 458–465. [CrossRef] [PubMed]
46. Robati, D. Pseudo-second-order kinetic equations for modeling adsorption systems for removal of lead ions using multi-walled carbon nanotube. *J. Nanostructure Chem.* **2013**, *3*, 55. [CrossRef]
47. Wu, F.C.; Tseng, R.L.; Juang, R.S. Characteristics of Elovic equation used for the analysis of adsorption kinetics in dye-chitosan systems. *Chem. Eng. J.* **2009**, *150*, 366–373. [CrossRef]
48. Wang, C.; Hu, X.; Chen, M.L.; Wu, Y.H. Total concentrations and fractions of Cd, Cr, Pb, Cu, Ni and Zn in sewage sludge municipal and industrial wastewater treatment plants. *J. Hazard. Mater.* **2005**, *B119*, 245–249. [CrossRef] [PubMed]
49. Yadanaparthi, S.K.P.; Graybill, D.; Wandruszka, R.V. Adsorbents for the removal of arsenic, cadmium, and lead from contaminated waters. *J. Hazard. Mater.* **2009**, *171*, 1–15. [CrossRef] [PubMed]